

160. A Kinetic Analysis of the Reaction Catalysed by (Hydroxymethyl)bilane Synthase¹⁾

by Annette C. Niemann^{a)}, Peter K. Matzinger^{b)}, and Alfons Hädener^{a)}*

^{a)} Institut für Organische Chemie der Universität Basel, St. Johannis-Ring 19, CH-4056 Basel

^{b)} F. Hoffmann-La Roche AG, Pharmaceutical Research – New Technologies, CH-4002 Basel

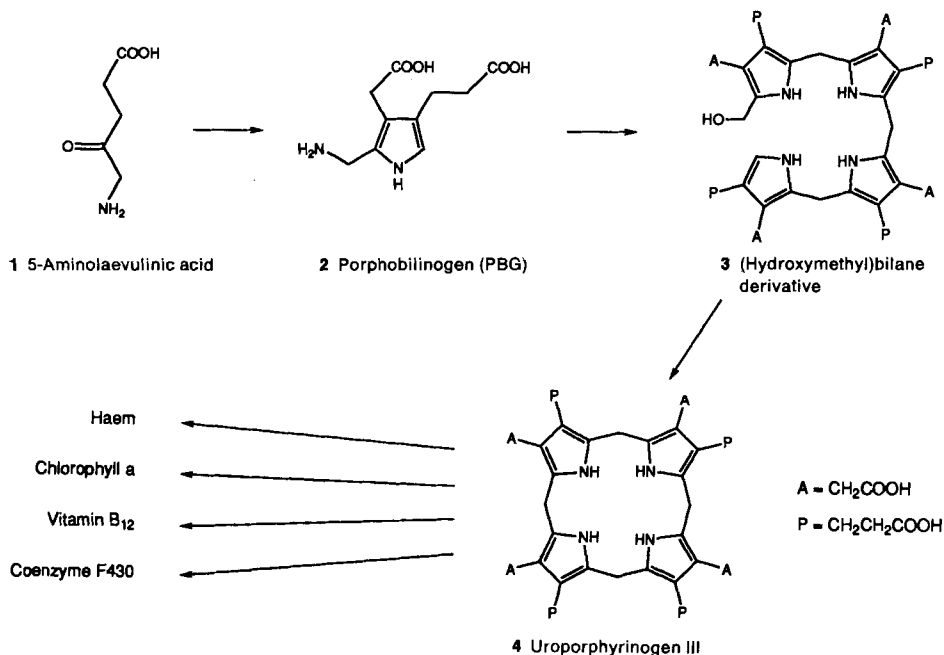
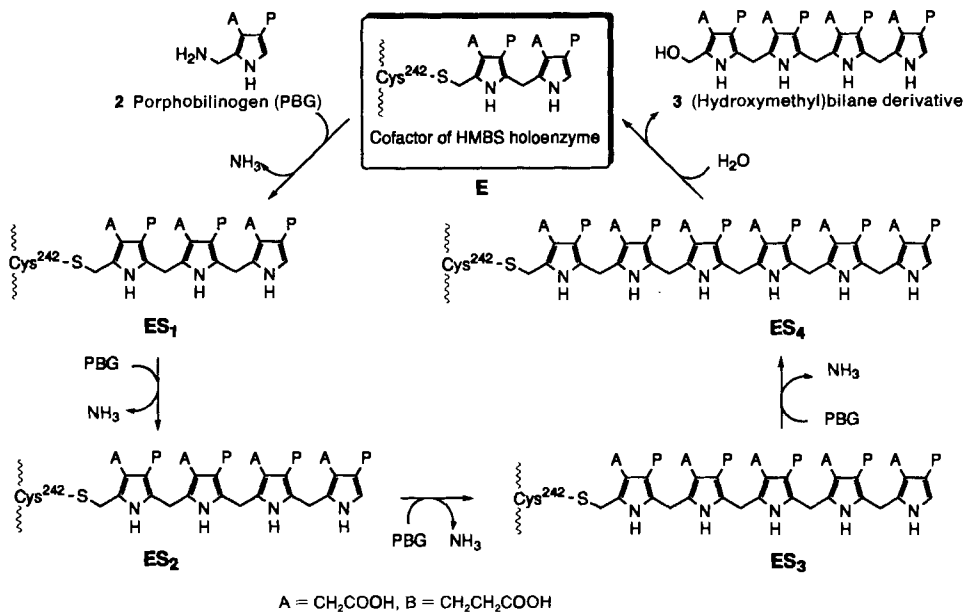
(15.VII.94)

(Hydroxymethyl)bilane synthase (HMBS) catalyses the conversion of porphobilinogen (**2**) into the (hydroxymethyl)bilane derivative **3**, a linear tetrapyrrolic intermediate in the biosynthesis of haem, chlorophyll, and related pigments. The conversion involves the sequential formation of four intermediate covalent enzyme-substrate complexes, before the product is released. We analysed the pre-steady-state kinetics of the formation of the complexes, taking advantage of their remarkable chemical stability allowing chromatographic separation. The experimental approach involved the generation of the complexes while HMBS was immobilised on an anion-exchange column. A solution being $0.2 K_m$ in substrate was pumped through the column during a time interval which was varied to sample the pre-steady-state period. Then, the enzyme and enzyme-substrate complexes were eluted and their proportions evaluated. A computer simulation of the pre-steady-state time course, in combination with a χ^2 fitting to the experimental data, allowed the specificity constants k_{cat}/K_m for the individual steps of the process to be derived. By repeating the analysis with variants of HMBS in which specific amino acids were replaced by others, we demonstrated that it is possible to trace the consequences of amino-acid replacements down to the individual steps of the reaction sequence. Since the positions of the amino acids concerned in the three-dimensional structure were known, detailed structure-function relationships become evident in this way.

Introduction. – (Hydroxymethyl)bilane synthase (HMBS, EC 4.3.1.8, also known as porphobilinogen deaminase) is an enzyme of the biosynthetic pathway leading to haem, chlorophyll, vitamin B₁₂, coenzyme F430, and related tetrapyrrolic pigments. It catalyses the conversion of four equivalents of porphobilinogen (PBG; **2**) into (hydroxymethyl)bilane derivative **3** and ammonia [1] [2] (*Scheme 1*).

HMBS is an enzyme converting PBG into products obeying *Michaelis-Menten* kinetics ($k_{cat} = 0.1 \text{ s}^{-1}$, $K_m = 5\text{--}10 \text{ }\mu\text{M}$ at pH 7.4 for HMBS from *Escherichia coli* [3]) [4] and displaying chemical reactivity of a polymerase [5]. The signal to stop polymerisation does not require any external factors, but is built into the HMBS molecule itself: as soon as four substrate molecules have been processed, the tetrameric product is released. To accomplish the assembly of the bilane, HMBS uses a unique dipyrin (= dipyrromethane) cofactor to which the growing chain remains covalently attached [6] [7] (see *Scheme 2*). The cofactor is in turn covalently bound to the enzyme *via* the S-atom of a cysteine residue (Cys-242 of the enzyme from *E. coli*). The HMBS apoenzyme, lacking the cofactor, is capable of assembling its own cofactor from two substrate molecules. Being derived from PBG (**2**), the cofactor can be isotopically labelled by

¹⁾ Abbreviations used: FPLC, fast-protein liquid chromatography; HMBS, (hydroxymethyl)bilane synthase; MAD, multiwavelength anomalous diffraction; PBG, porphobilinogen; SeMet, selenomethionine.

Scheme 1. *The Biosynthesis of Haem, Chlorophylls, Vitamin B₁₂, and Related Macrocycles*Scheme 2. *State Transitions of HMBS from E. coli during the Conversion of PBG (2) to (Hydroxymethyl)bilane Derivative 3*

biosynthetic incorporation of labelled 5-aminolaevulinic acid (**1**), and the fact that such labels are not released during normal catalytic turnover implies that the cofactor remains in place throughout the catalytic cycle and does not turn over [8]. The reaction cycle of HMBS catalysis can thus be summarised as shown in *Scheme 2*.

The intermediates ES_i ($i = 1, 2, 3, 4$) of the catalytic reaction cycle shown in *Scheme 2* were first characterised by *Anderson* and *Desnick* who noted that HMBS from human erythrocytes forms moderately stable complexes with its substrate in stoichiometric ratios 1:1, 1:2, 1:3, and 1:4, and that these can be separated by anion-exchange chromatography or by electrophoresis [9]. Experiments with HMBS from *Euglena gracilis* and *E. coli* confirmed these results [10–12]. The ES_i complexes can routinely be generated and detected by mixing HMBS (in μmol quantities) with PBG in molar ratios of 1:1 to 1:10 followed by ion-exchange chromatography on a *MonoQ* anion-exchange support [11] [8]. However, the ES_4 complex which had readily been detected with human HMBS was not observed with the algal and bacterial enzymes under normal conditions. The ES_4 complex of the enzyme from *E. gracilis* can be generated by mixing HMBS with equimolar amounts of (hydroxymethyl)bilane derivative **3** and is only stable in the absence of PBG (**2**) [5]. The ES_4 complex of the enzyme from *E. coli* could only be observed with certain site-directed mutant variants that showed no turnover activity [13].

To investigate the formation of the enzyme-substrate complexes and the mechanisms for assembly of the oligopyrrolic chain and release of (hydroxymethyl)bilane derivative **3**, it seems attractive to take advantage of the stability of the complexes and to assay their formation in a quantitative way. An early experiment of this kind was carried out in 1979, when HMBS from *E. gracilis* was first mixed with a deficiency of unlabelled PBG (**2**) and then with an excess of $[11-^{13}\text{C}]$ PBG to establish the order of assembly of the four pyrrole rings and the timing of the rearrangement of ring D during the biosynthesis of uroporphyrinogen III (**4**) [14]. Later, the dependence of the relative proportions of complexes formed from *E. coli* HMBS on the equivalent amount of added PBG was studied in detail [8]. Here, the aim was to maximise the yield of ES_1 and ES_2 after addition of $[11-^{13}\text{C}]$ PBG in order to establish by NMR the nature of the functional group to which the first PBG unit is covalently bound.

Similar techniques were used to assess the influence of site-directed amino-acid replacements on the mechanisms of chain elongation and product release [13] [15]. Again, the independent variable in these assays was either the initial concentration of PBG (**2**) or the number of equivalents of **2** used with respect to HMBS.

A fundamental difficulty is encountered, however, if kinetic parameters were to be deduced from such experiments. Whereas the relative amounts of enzyme and **2** can be readily adjusted, and it is easy to control the initial concentration of **2**, the behaviour of the system becomes more complicated as substrate is consumed in the course of the reaction. The substrate concentration may initially saturate the enzyme, then decrease gradually to K_m , and reach values well below K_m at the time when the reaction is stopped and the mixture is chromatographed. Furthermore, product inhibition may interfere with the turnover, and it seems difficult to determine whether all **2** has been finally consumed. Hence, it is practically impossible to reconstruct the time course of the formation of the complexes from merely looking at the final relative proportions of complexes.

There is, however, an elegant way to overcome these limitations. We show in this paper that by allowing the complexes to form under readily controlled conditions while

HMBS is immobilised on a stationary phase, it is possible to determine kinetic specificity constants for individual steps of the sequential reaction. Furthermore, by repeating the kinetic analysis with both selenomethionine-labelled HMBS ($[(\text{SeMet})_6]\text{HMBS}$) and a variant of HMBS obtained by site-directed mutagenesis for which Lys-59 is replaced by Gln ($[\text{Gln}^{59}]\text{HMBS}$), we show that it is possible to trace the consequences of amino-acid replacements down to individual steps of the reaction sequence. As the three-dimensional structure of HMBS is known [16], detailed structure-function relationships may become evident in this way.

Results and Discussion. – 1. *Generation of the Enzyme-Substrate Complexes on a Solid Support.* The fact that the ES_i complexes may be separated by chromatography on an anion-exchange support (*MonoQ*) using a NaCl gradient led us to the idea to generate the complexes while HMBS is already loaded on the column, immediately before the start of the gradient. This may be accomplished by pumping a solution of PBG (**2**) through the column under conditions where **2** is eluted but not HMBS. Fortunately, these conditions exist, since at the pH optimum of HMBS, the overall negative charge of **2** is much smaller than that of HMBS. To find the precise conditions, the retention volumes of **2** and HMBS on a *MonoQ HR5/5* column were determined as a function of the concentration of NaCl in the mobile phase. We found that using 88 mM NaCl in 15 mM *Tris*·HCl at the pH optimum of wild-type enzyme (pH 7.5 [17]), **2** was eluted with 1.22 void volume, whereas HMBS was almost completely retained by the column.

To demonstrate that HMBS, immobilised in this way, can form substrate complexes, an ordinary FPLC¹) was used. First, an aliquot of enzyme was immobilised on the column using the mobile phase mentioned above. A large sample loop containing a solution of PBG (**2**) in the same solvent was then connected to the injection valve (Fig. 1, a). By switching the valve, the solution of **2** was pumped through the column and the enzyme allowed to form complexes with the substrate under controlled conditions (Fig. 1, b). After a certain time, the valve was switched back, and a NaCl gradient was run to elute and separate the enzyme-substrate complexes (Fig. 1, c). Indeed, the enzyme-substrate complexes had been generated, and their proportions could be measured by on-line integration (Fig. 1, d).

In principle, the peak proportions observed in this way contain information about the relative rates of formation of each of the enzyme-substrate complexes and the rate of regeneration of the holoenzyme, when the product, (hydroxymethyl)bilane derivative **3**, is released. By sensibly changing the experimental parameters, it seemed possible to gain enough data (i.e., different peak proportions) to estimate these rates.

2. *Pre-Steady-State Kinetic Analysis of Immobilised HMBS at Low Substrate Concentration.* Several parameters can affect the observed proportions of free enzyme and enzyme-substrate complexes: the amount of enzyme loaded, the concentration of PBG (**2**), the flow rate, and the contact time (the time during which the PBG solution is pumped through the column). A closer examination reveals that all parameters except one should be kept constant.

Amount of Protein Loaded. Previous work [5] established that HMBS from *E. gracilis* is competitively inhibited by (hydroxymethyl)bilane derivative **3**. Since, in addition, **3** itself is converted into uroporphyrinogen I in a nonenzymatic unimolecular process, any variation of the HMBS concentration in kinetic experiments will lead to different appar-

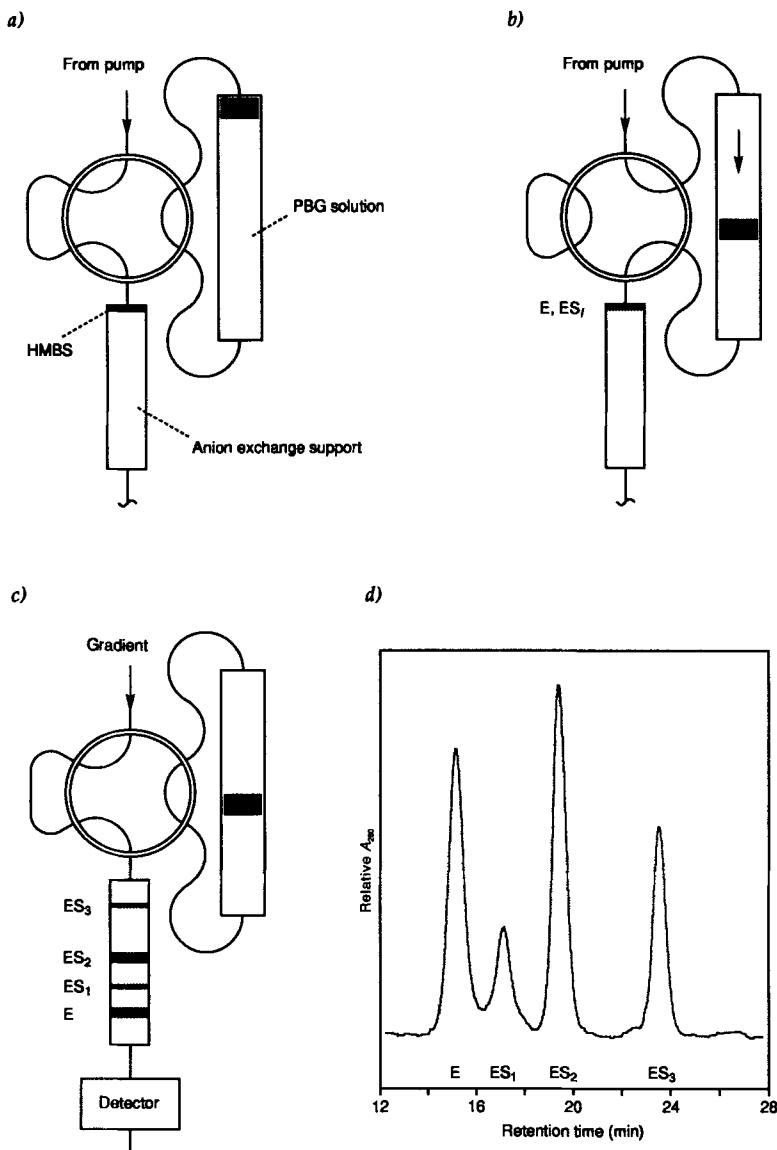


Fig. 1. Experimental set-up for the generation of immobilised enzyme-substrate complexes on a MonoQ anion-exchange support. *a*) Wild-type HMBS (0.10 mg, 2.94 nmol) was loaded onto a MonoQ HR 5/5 column using 88 mM NaCl in 15 mM Tris · HCl (pH 7.5) as mobile phase. *b*) At room temperature, a solution of PBG (**2**; 1.46 μ M, ca. 0.2 K_m) in the same buffer was pumped through the column during 4.0 min at 3.0 ml/min (a bung prevents mixing of mobile phase and PBG solution). *c*) *d*) The complexes were then eluted by applying an ionic-strength gradient (88–350 mM NaCl in 30 ml), detected at 280 nm, and their proportions estimated by on-line integration.

ent kinetic parameters [5]. Although it seems possible to separate effects of unimolecular decomposition of **3**, of competitive inhibition of HMBS by **3**, and of true kinetic parameters of the enzymatic reaction sequence by computer simulation of the entire process, we decided to keep the amount of enzyme loaded constant. This precaution will minimise any unwanted monitoring of second-order effects as well, e.g., local variations of pH due to variable loading of protein [18].

Concentration of PBG (2). [PBG] should be kept well below K_m of HMBS (i.e., not higher than $0.2 K_m$), for the following reason. For substrate concentrations above ca. $0.2 K_m$, saturation of the enzyme becomes important, i.e., the first-order dependence of rate on substrate concentration at very low concentrations is no longer valid. Mechanistically, this means that a significant portion of the enzyme is present as a *Michaelis* complex. In our case, significant amounts of *Michaelis* complexes (denoted ES, ES₁S, ES₂S, ES₃S, see below) between **2** and either free holoenzyme E or ES_i species would be accumulated. When the substrate flow is interrupted, the decomposition of these *Michaelis* complexes, either forward or backward, would alter the proportions of stable covalent complexes and free enzyme in an unpredictable way. Keeping, therefore, [PBG] well below K_m , the second requirement is that it should not be varied for reasons related to diffusion control.

Flow Rate. For the same reasons, the flow rate should be kept constant as well. A special feature of the kinetics of immobilised enzymes is the importance of diffusion-controlled processes [18]. These are especially important at low substrate concentration, and results obtained by varying the substrate concentration under these conditions may monitor kinetic parameters related to diffusion rather than kinetic parameters of the enzyme. The contribution of diffusional control to the overall behaviour of the heterogeneously catalysed reaction mixture is strongly dependent on the flow rate at low flow rates, on the particle size of the solid support, and on the size and shape of the internal pores of the particles. To prevent masking of true enzyme kinetics by external diffusional control, flow rates should be kept high. *Buchholz* concluded that external mass transfer had a minor influence on the overall reaction rate, when the relative velocity of the fluid and the beads was $0.1\text{--}1\text{ cm s}^{-1}$ [18]. The corresponding quantity for a *MonoQ HR5/5* column operated at 3 ml/min is ca. 0.6 cm s^{-1} (see *Exper. Part*). For particular systems, critical velocities between 0.024 and 0.4 cm s^{-1} were reported [18]. It seems, therefore, wise to keep the flow rate high and constant in order to avoid possible monitoring of diffusion effects.

Contact Time. This is the parameter to be varied. Given a known amount of HMBS immobilised on *MonoQ HR 5/5*, a solution of **2** at a fixed concentration well below K_m of the enzyme is started to be pumped through the column at a constant flow rate. After some time, a steady state will be reached in which all enzyme species including free enzyme E, ES_i, and the *Michaelis* complexes are formed and processed at constant rate. The substrate concentration (now unknown) will also be at steady state, because substrate is permanently resupplied as it is taken up by the enzyme. The same is even true for the product concentration, since as (hydroxymethyl)bilane derivative **3** is being formed, it will decay by cyclization to form uroporphyrinogen **1** which will slowly accumulate.

If the substrate flow is then interrupted, i.e. the flow switched to mobile phase without substrate, the *Michaelis* complexes (ES, ES₁S, ES₂S, ES₃S, EP) will decay to give the stable enzyme species (E, ES₁, ES₂, ES₃, ES₄) without noticeably changing the proportions of the latter with respect to their proportions at steady state (note again the requirement to use

low substrate concentrations for this reason). The stable enzyme species may then be eluted by applying a NaCl gradient and their proportions be determined.

HMBS has the unique feature to be a rather slow enzyme. Whereas values of k_{cat} lie between 1 and 10^7 s^{-1} for most enzymes [19], k_{cat} of HMBS from *E. coli* is ca. 0.1 s^{-1} [3]. In addition, the supply of **2** in terms of mol per mol of immobilised HMBS and unit time will be relatively low (cf. the legend to Fig. 1). The build-up of the steady state mentioned above is, therefore, expected to occur on a time scale in the order of minutes. This opens up the possibility of interrupting the substrate flow, before the steady state is reached. Intermediate proportions of stable enzyme species on the way to the steady-state proportions can then be measured and plotted as a function of time.

In summary, the experimental approach to examine the pre-steady-state period consists of a series of independent experiments each with identical starting conditions (amount of protein loaded, concentration of PBG, flow rate), but different contact times.

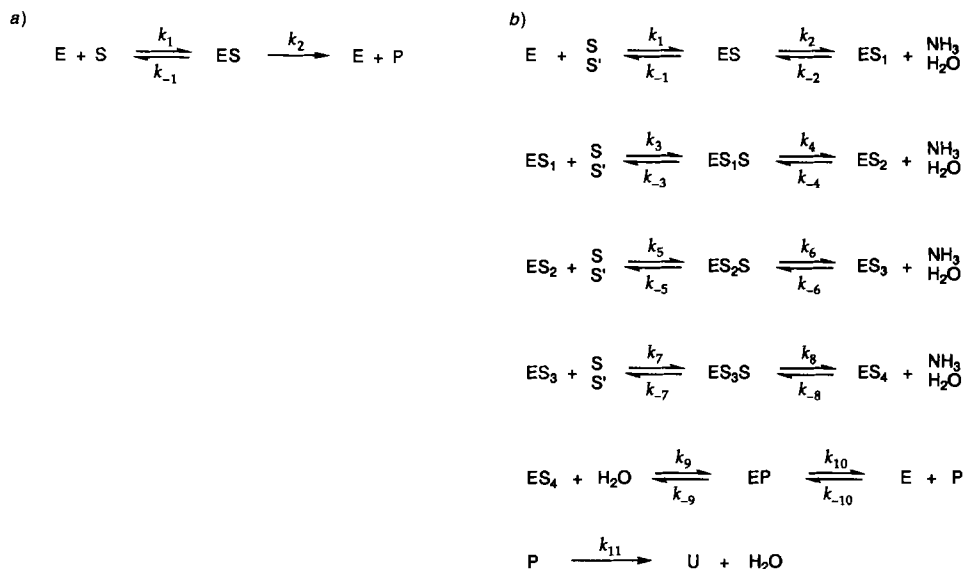
This concept was put into practice by repeating the experiment shown in Fig. 1 using various contact times from 15 s up to 11 min. As expected from previous work on the enzyme-substrate complexes of HMBS from *E. coli*, the ES_4 complex was never detected in these experiments. The integrated areas summed over the 4 peaks remained constant, within experimental error, over the entire range of contact times. Control experiments in which mobile phase without **2** was pumped over the immobilised enzyme gave rise to a single peak, the area of which was equal, within experimental error, to the sum of the areas of the 4 peaks in the other experiments. Taken together, these findings imply that ES_4 or indeed any other undetected enzyme species, if present, had been formed in negligible quantities only.

The time course of the build-up of the steady state thus obtained is shown in Fig. 2, a (see below). To derive the underlying kinetic parameters for each of the observable steps in the enzymic conversion of **2** into **3** from the measured data, a reasonable model of the kinetic reaction scheme was first established and then a computer simulation of the experimental process run using an initial set of kinetic parameters. Using a standard simplex optimisation procedure [20] [21], the outcome of the simulation was gradually improved by adjusting the kinetic parameters.

3. A Model of the Kinetic Reaction Scheme. Since the overall reaction catalysed by HMBS exhibits *Michaelis-Menten* kinetics, it can be represented by the general two-step mechanism according to Briggs and Haldane [22] (Scheme 3a). Without losing overall *Michaelis-Menten* behaviour, this mechanism can be extended to include four sequential two-step reactions and an additional unimolecular step in which the product is released [4]. However, further evidence has accumulated in the meantime, and the mechanism shown in Scheme 3, b may be proposed for the reaction catalysed by HMBS.

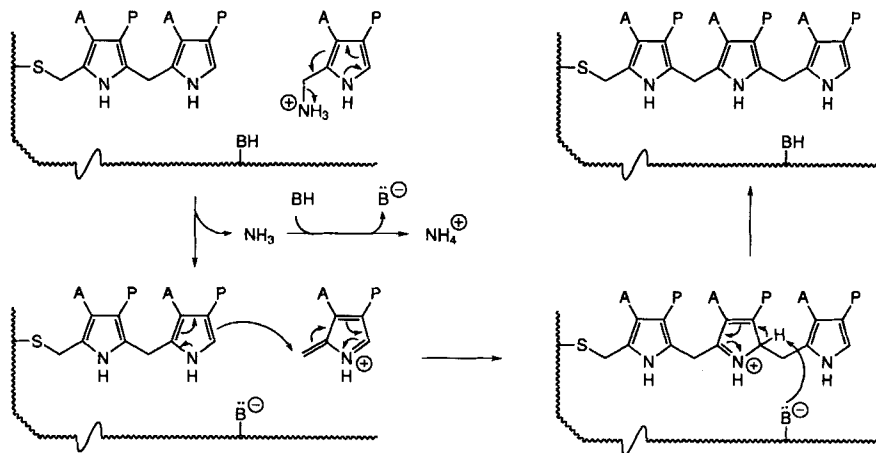
The mechanism is designed to be as general as possible but to include known features at the same time. Each of the five consecutive reactions is represented by a general two-step reversible mechanism. The *Michaelis* complexes, formally denoted ES, ES_2 and EP, probably represent more than one intermediate species along the sequence of steps in which a single new PBG unit is attached to the growing chain (Scheme 4), or in which the product is released from ES_4 (Scheme 5) [8] [23]. Reversibility is included for all reactions to keep the model as general as possible and to allow for the fact that the covalent complexes of HMBS from *E. coli* can be interconverted by incubation at 37° for 15 min [24]. Interconversion is likely to proceed *via* hydrolytic cleavage at the terminal pyrrole

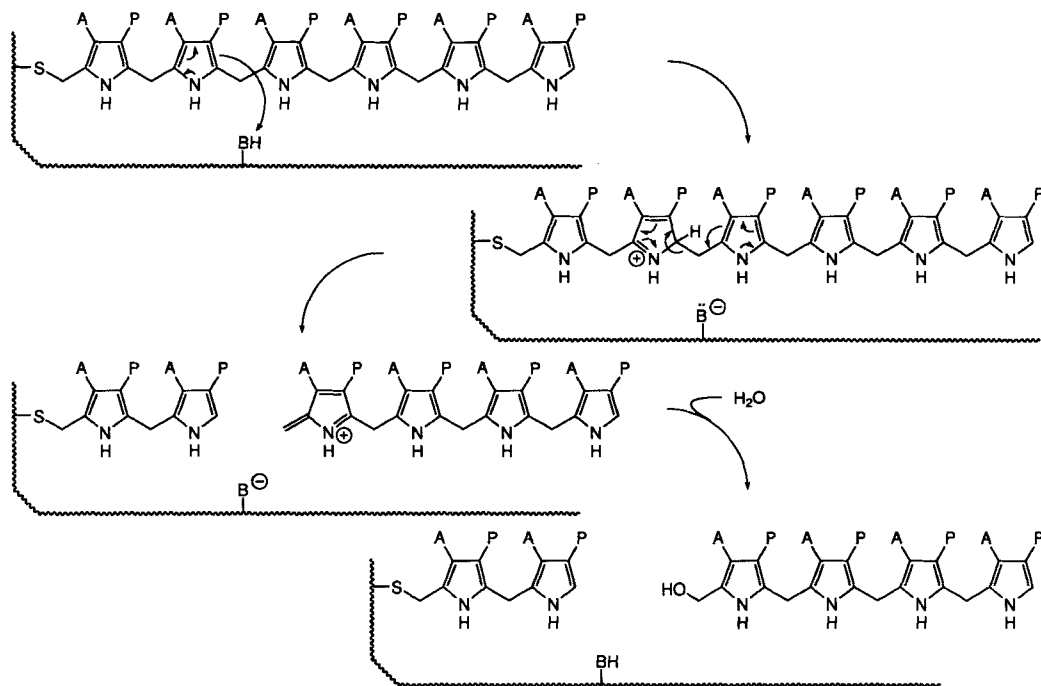
Scheme 3. a) *General Two-Step Mechanism According to Briggs and Haldane* [22]. b) *Sequential Mechanism Characterising the Conversion of PBG (2) to (Hydroxymethyl)bilane Derivative 3 Catalysed by HMBS and the Unimolecular Cyclisation of 3 to Uroporphyrinogen I*



S = substrate (PBG; 2); S' = hydroxy analogue of PBG; P = product ((hydroxymethyl)bilane derivative 3); E, ES₁, ES₂, ES₃, ES₄ = stable (covalent) enzyme-substrate complexes; ES, ES₁S, ES₂S, ES₃S, EP = *Michaelis* complexes; U = uroporphyrinogen I; k_i = rate constants

Scheme 4. *Model for the Chain-Assembly Mechanism Used by HMBS for the Conversion of PBG (2) to (Hydroxymethyl)bilane Derivative 3*. The attachment of the first PBG unit to the dipyrrole cofactor is shown, representative of three chain-elongation steps which are to follow.



Scheme 5. Model for the Mechanism of the Release of (Hydroxymethyl)bilane Derivative **3** from HMBS after Assembly of a Hexapyrrolic Chain

unit. This process is expected to generate a hydroxy analogue of PBG (denoted S' in Scheme 3), a compound that is known to be a good substrate for HMBS [25]. With respect to our experimental set-up, however, it must be emphasised that in the absence of substrate, the complexes are stable at room temperature on *MonoQ*, at least during the time needed for chromatography (25 min), as illustrated by the nearly symmetrical peak shapes observed (Fig. 1, d). It is, therefore, very likely that k_{-2} , k_{-4} , k_{-6} , and k_{-8} take on values close to zero. For the last reaction in which the product is released from ES_4 , reversibility is included to take into account that the stable ES_4 complex of HMBS from *E. gracilis* may be set-up by mixing the enzyme with synthetic (hydroxymethyl)bilane derivative **3** in a molar ratio of 1:1 [5]. A *Michaelis* complex EP is included in this reaction, since the formation of ES_4 from $E + P$ is chemically analogous to the formation of ES_1 from $E + S$. The unimolecular conversion of **3** into uroporphyrinogen I is added to the scheme, because it controls the concentration of **3** during the pre-steady-state period. A half-life of ca. 5 min at 37° and pH 8.25 was reported for **3** [26]. This corresponds to a value for k_{11} of $2.3 \cdot 10^{-3} \text{ s}^{-1}$ under these conditions.

The steady-state assumption can then be applied to the concentrations of the *Michaelis* complexes and of the ES_4 complex. This means that during any very small time increment of the pre-steady-state period, each of the consecutive reactions shown in Scheme 3 is considered to be at steady state with respect to the concentrations $[ES]$, $[ES_2]$, $[EP]$, and $[ES_4]$ at that particular time. The resulting six equations are used to eliminate

the concentrations of the *Michaelis* complexes and of the ES_4 complex in the rate equations for the stable species. Thus *Eqns. 1–6* are obtained

$$d[E]/dt = c_{11}[ES_3][S] + c_2[ES_1] - c_1[E][S] - c_{12}[E][P] \quad (1)$$

$$d[ES_1]/dt = c_1[E][S] + c_4[ES_2] - c_3[ES_1][S] - c_2[ES_1] \quad (2)$$

$$d[ES_2]/dt = c_3[ES_1][S] + c_6[ES_3] - c_5[ES_2][S] - c_4[ES_2] \quad (3)$$

$$d[ES_3]/dt = c_5[ES_2][S] + c_{12}[E][P] - c_{11}[ES_3][S] - c_6[ES_3] \quad (4)$$

$$d[S]/dt = c_2[ES_1] + c_4[ES_2] + c_6[ES_3] + c_{12}[E][P] \\ - [S](c_1[E] + c_3[ES_1] + c_5[ES_2] + c_{11}[ES_3]) + FV_0^{-1}([PBG] - [S]\sigma) \quad (5)$$

$$d[P]/dt = c_{11}[ES_3][S] - c_{12}[E][P] - [P](k_{11} + F\rho V_0^{-1}) \quad (6)$$

where F is the flow rate, $[PBG]$ is the initial concentration of substrate (before the substrate solution enters the column), and V_0 is an auxiliary variable denoting a formal volume in which the reaction takes place (all concentrations other than $[PBG]$ are formal with respect to this volume). The factors σ and ρ are coefficients related to the retention characteristics of PBG (**2**) and (hydroxymethyl)bilane derivative **3** on *MonoQ* at the experimental conditions. It can be shown (see *Exper. Part*) that σ is equal to the void volume of the chromatographic column divided by the retention volume of PBG ($\sigma = 0.821$ at the conditions described in the legend to *Fig. 1*). An analogous definition applies to ρ , and both factors can assume values between zero and one in general. In our set-up the value of ρ is very close to zero, since **3** is completely retained by *MonoQ* during the reaction. This follows from the observation that accumulated **3** and uroporphyrinogen **1** can be washed out after the elution of the enzyme-substrate complexes by injection of 1 ml of 2M NaCl (see below).

In all equations, c_i represents collections of rate constants according to *Eqn. 7*.

$$c_i = \frac{k_i k_{(i+1)}}{k_{-i} + k_{(i+1)}} \quad (i = 1, 3, 5, 7, 9), \quad \text{e.g. } c_1 = \frac{k_1 k_2}{k_{-1} + k_2}; \quad c_{11} = \frac{c_7 c_9}{c_8 + c_9}; \\ c_j = \frac{k_{-j} k_{-(j-1)}}{k_{-j-1} + k_j} \quad (j = 2, 4, 6, 8, 10), \quad \text{e.g. } c_2 = \frac{k_{-1} k_{-2}}{k_{-1} + k_2}; \quad c_{12} = \frac{c_8 c_{10}}{c_8 + c_9} \quad (7)$$

Note that the specificity constant k_{cat}/K_m for the general two-step mechanism mentioned earlier is equal to $k_1 k_2 / (k_{-1} + k_2)$ [22]. Therefore, the constants c_i ($i = \text{odd}$) represent k_{cat}/K_m for each of the consecutive forward reactions, whereas c_j ($j = \text{even}$) represent an analogous quantity for the reverse reactions.

By applying the steady-state assumption to the concentrations of the *Michaelis* complexes as described above, all information about k_{cat} and K_m values separately is lost. Only the ratios k_{cat}/K_m are retained and may be extracted by simulation/optimisation procedures. However, this is in keeping with the experimental design which requires the substrate concentration to be low with respect to K_m . At these conditions, any attempts to measure k_{cat} and K_m separately would fail since only the initial slope in the plot of the *Michaelis-Menten* equation is being considered, where *Eqn. 8*

$$v \approx k_{\text{cat}} K_m^{-1} E_0 [S] \quad (8)$$

is valid (E_0 = total enzyme concentration). Hence, the rate shows first-order dependences on both the enzyme and substrate, or second-order kinetics overall [22].

According to textbooks, K_m is an apparent dissociation constant that may be treated as the overall dissociation constant of all enzyme-bound species (see, e.g., [19]). It is important to realise that this rule must be cautiously applied to the HMBS mechanism. Here, 'all enzyme-bound species' include only those which cannot react with substrate. Therefore, ES_1 , and ES_2 , and ES_3 must be treated as 'free enzyme', since they can react with S like the holoenzyme E.

4. Simulation and Optimisation Procedures. Based on the rate equations, a computer programme for the simulation of the pre-steady-state course was written. The software package ModelWorks [27] within the environment RAMSES [28] was used to develop and run the programme which is written in Modula-2 [29]. In finding an initial set of values for the constants c_i , we took advantage of the fact that, based on the first four rate equations, the steady-state proportions of the enzyme species are related to the constants c_i in a simple way. Thus, given $d[E]/dt = 0$ and $d[ES_i]/dt = 0$ ($i = 1, 2, 3$) as required for the steady state and assuming $c_j = 0$ ($j = 2, 4, 6, 8$), we get Eqn. 9

$$c_3/c_1 = [E]/[ES_1], c_5/c_1 = [E]/[ES_2], c_{11}/c_1 = [E]/[ES_3] \quad (9)$$

where the concentrations of enzyme species are those at steady state (one of the first four rate equations is redundant in this case). This is equivalent to knowing the values of c_3 , c_5 , and c_{11} relative to c_1 (see Table, relative k_{cat}/K_m values).

Table. *Specificity Constants in HMBS Catalysis.* Data are given for immobilised enzymes operating at pH 7.5 and 22°.

Step	Specificity constants k_{cat}/K_m					
	Wild-type HMBS		[(SeMet) ₆]HMBS		[Gln ⁵⁹]HMBS ^{a)}	
	relative	M ⁻¹ s ⁻¹	relative	M ⁻¹ s ⁻¹	relative	M ⁻¹ s ⁻¹
E → ES ₁	1.00	30 400 13 600	1.00	27 100	1.00	41 600
ES ₁ → ES ₂	2.46 2.66	74 700 36 100	2.19	59 400	2.41	100 300
ES ₂ → ES ₃	0.945 0.982	28 700 13 300	1.59	43 100	0.0176	733
ES ₃ → E	1.42 1.57	43 200 21 300	2.71	73 300	0.00388	162
Overall		9 600 4 480		11 030		135

^{a)} An unreactive fraction of enzyme (10.5%) and the hydrolysis $ES_2 \rightarrow ES_1$ at 0.0114 s⁻¹ were optimal in this simulation.

The remaining parameters were assigned the following values (see above and Fig. 1): $F = 3$ ml/min, $[PBG] = 1.46 \mu\text{M}$, $k_{11} = 2.31 \cdot 10^{-3} \text{ s}^{-1}$, $E_0 = 2.94 \text{ nmol}/V_0$, $\sigma = 0.821$, and $\rho = 0$; the formal volume V_0 was arbitrarily set to 200 μl . The settings of V_0 and of k_{11} had no significant effect on the outcome of the simulation.

Then, starting with the total enzyme concentration E_0 , the build-up of the steady state was simulated over the preselected time interval 0 to 670 s. The deviations of the progress

curves for each enzyme species from the corresponding experimental data points, divided by the corresponding standard deviations, were squared and added up to give a measure χ^2 of the quality of the fit [30]. Subsequently, the values of c_1 , c_3 , c_5 , and c_{11} were adjusted by simplex optimisation [20] in such a way that the value of χ^2 was a minimum. The simulated build-up of the steady-state proportions of the enzyme species, as obtained in this way, is shown in Fig. 2a. A rapid decrease of free enzyme in favour of the formation of the enzyme-substrate complexes dominates the early pre-steady-state period, until after *ca.* 5 min a steady state is reached which is characterised by the presence of E, ES₁, ES₂, and ES₃ in constant proportions and by 1.45 ± 0.02 equiv. of PBG being attached to the enzyme on average.

It is noteworthy that the proportions of E, ES₁, ES₂, and ES₃ at steady state, and hence the *relative* specificity constants k_{cat}/K_m for the individual steps of the reaction were reproduced with considerable accuracy when the entire experiment was repeated with HMBS purified from cells of an independent fermentation broth (*Table*). In contrast, the *absolute* values for the specificity constants scatter considerably, a fact that is also encountered with determinations of overall apparent k_{cat}/K_m in solution [3]. The latter constant was found to be $9340 \pm 4630 \text{ M}^{-1} \text{ s}^{-1}$ ($n = 6$) for the wild-type enzyme operating at pH 7.4 and 22°. This value compares favourably with the overall specificity constant that can be derived from the optimised simulation of the pre-steady-state reaction course, using *Eqn. 10*

$$\left(\frac{k_{\text{cat}}}{K_m} \right)_{\text{overall}} = \frac{c_{11}[\text{ES}_3]}{E_0} = \frac{F}{4V_0 E_0} \left(\frac{[\text{PBG}]}{[\text{S}]} - \sigma \right), \quad (10)$$

where [ES₃] and [S] are concentrations at steady state. In two independent experiments, values of $9600 \text{ M}^{-1} \text{ s}^{-1}$ and $4480 \text{ M}^{-1} \text{ s}^{-1}$ were obtained for wild-type HMBS (*Table*).

Due to its large overall negative charge at pH 7.5 (hydroxymethyl)bilane derivative **3** is trapped on the anion-exchange support as it is formed during the reaction. It is even retained during the elution of the enzyme-substrate complexes. The total amount of product that had been formed in individual experiments could, therefore, easily be determined by collecting **3** as well as uroporphyrinogen I that may have been formed by cyclisation after the elution of the enzyme-substrate complexes. This was accomplished by repeated injections of small portions of 2M NaCl. The eluted compounds were determined spectrophotometrically after conversion to uroporphyrin I by treatment with CCl₃COOH and I₂ [4]. The amount of product formed after 240, 360, and 660 s, as determined in this way, matched the amount predicted by the simulation of the process within experimental error. For this simulation, k_{11} was set to zero to allow the monitoring of the accumulation of the total amount of **3**.

It has been mentioned that measurements should be made at substrate concentrations low with respect to K_m . The question is raised as to whether the actual concentration of substrate (formal with respect to V_0) will increase (due to slight retention of PBG (**2**) on *MonoQ* under the conditions used) or decrease (due to the consumption of **2** as soon as it encounters the immobilised enzyme) in the course of the experiment. The simulation of the process in the case of wild-type HMBS reveals that the latter effect prevails. Within a few s, the actual concentration of substrate reaches a steady state at *ca.* 1/2 to 1/3 of the external PBG concentration [PBG].

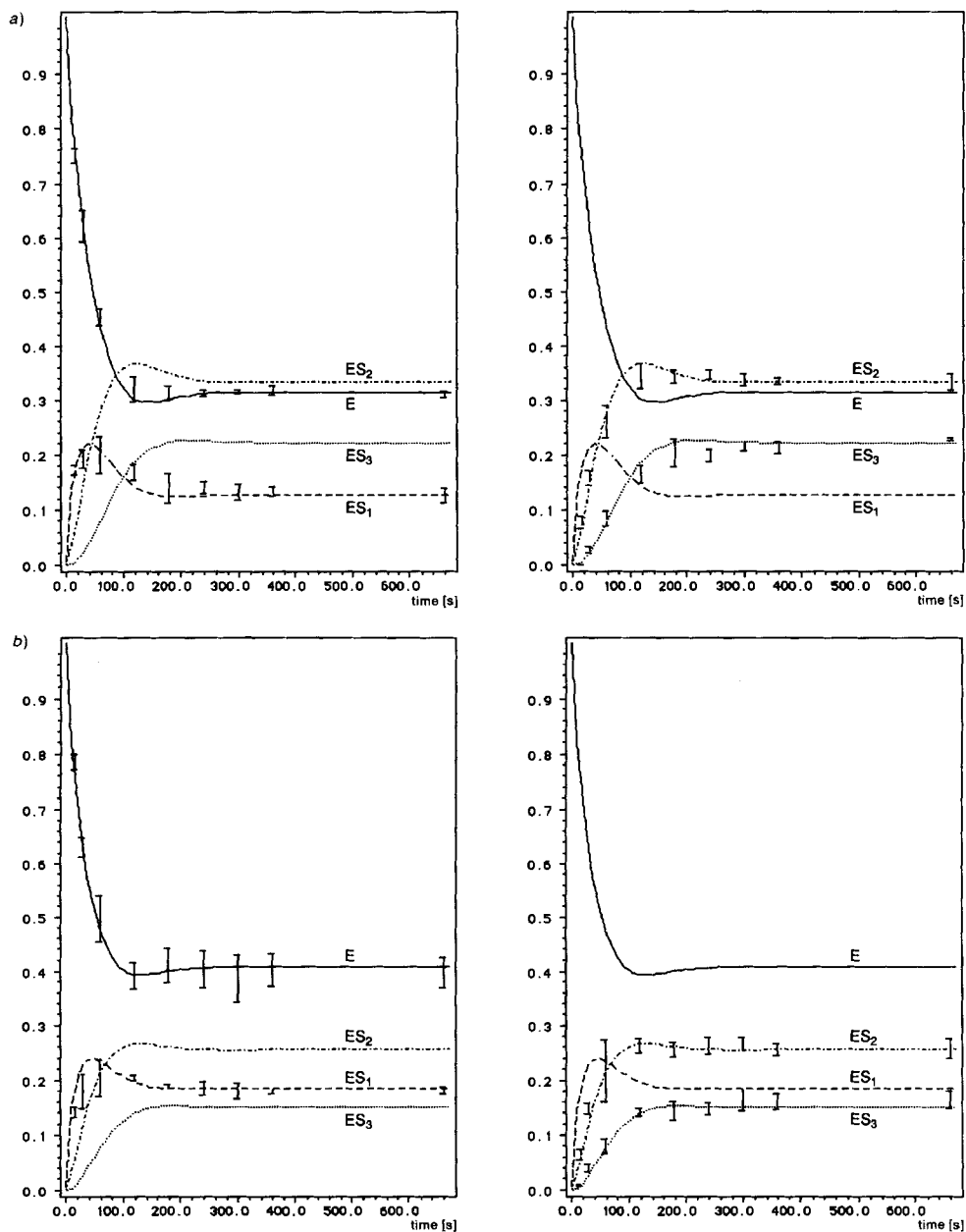
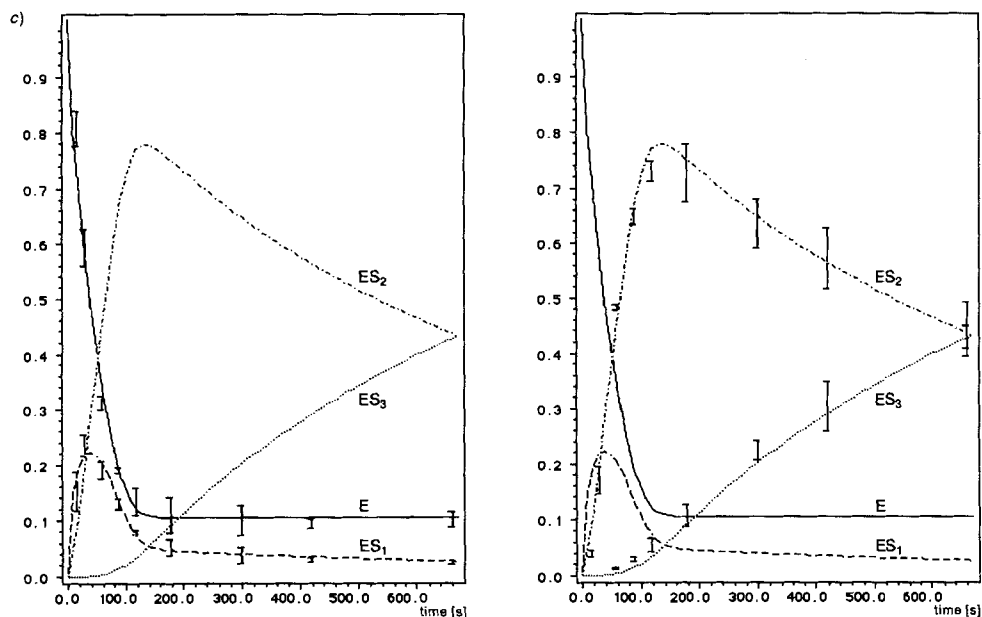


Fig. 2. Measured and simulated pre-steady-state time dependence of the relative concentrations of the stable enzyme species E , ES_1 , ES_2 , and ES_3 : a) Wild-type HMBS, b) $[(SeMet)_6]HMBS$ and c) $[Gln^{59}]HMBS$. In the case of $[Gln^{59}]HMBS$, 5 measurements were made between 900 s and 3600 s in addition to the 9 measurements shown; the simulated time course shown in Fig. 2, c is the result of an optimisation in which all measurements were considered. For the sake of clarity each figure is split into two parts showing the measured proportions of E , ES_1 (left-hand) and ES_2 , ES_3 (right-hand) separately, along with the optimised simulated time courses. Standard deviations are drawn as error bars.

Fig. 2 (cont.)



5. *Kinetics of Mutant HMBS Variants. General Considerations.* It seems attractive to trace the consequences of amino-acid replacements down to individual steps of the reaction sequence by repeating the pre-steady-state kinetic analysis with site-directed mutant variants of HMBS. A single site mutation could affect all rates proportionally, or it could specifically alter one rate leaving the others unaffected, or there could be a mixed and more complicated influence.

A number of site-directed mutant variants of HMBS from *E. coli* were described in the literature [3] [13] [15]. Many of them completely lack any activity in converting PBG to product. In these cases, the original residues concerned play an absolutely essential role in the catalytic mechanism. A representative example is the replacement of Cys-242 by Ser ([Ser²⁴²]HMBS). The resulting mutant enzyme lacks the anchor to which the dipyrin cofactor has to be attached and indeed shows no activity [31]. Other deleterious replacements include the one of arginine residues at positions 11, 131, 132, and 155 by leucine or histidine, but in these cases, the mechanistic reasons are not well understood yet. It is obvious that pre-steady-state analyses are not applicable in cases where amino-acid replacements are deleterious.

Other amino-acid replacements (Lys-59 by Gln, Arg-149 by Leu, Arg-176 by Leu, Arg-232 by Leu) affect the enzymatic activity of HMBS less seriously, allowing some turnover of PBG into product. These replacements affect both K_m and k_{cat} , except the replacement of Lys-59 by Gln which affects overall K_m only but not k_{cat} [3]. The effect of this replacement on the mechanism of catalysis might indeed be very specific.

Yet other replacements do not seem to affect catalysis at all. This class is well represented by [(SeMet)₆]HMBS, a variant in which all (six) methionine residues are replaced by selenomethionine (SeMet). The overall values of the steady-state kinetic

parameters K_m and k_{cat} for $[(\text{SeMet})_6]\text{HMBS}$ are very similar to those of wild-type enzyme [32].

To test the pre-steady-state analysis of mutant HMBS variants, $[\text{Gln}^{59}]\text{HMBS}$ and $[(\text{SeMet})_6]\text{HMBS}$ were chosen as representative examples. The enzymes were over-expressed in the corresponding strains of *E. coli* and purified as reported earlier [3] [32]. The experimental set-up for the kinetic analysis and the parameters used were the same as described above for wild-type HMBS.

$[\text{Gln}^{59}]\text{HMBS}$. Strikingly, it takes considerably longer until a steady state is reached in this case (Fig. 2c). Both the initial disappearance of E and the curve for ES_1 approximately follow a course that is also exhibited by wild-type HMBS. Both the time and the amplitude of the maximum of the curve for ES_1 are roughly equal, and the steady-state values of E and ES_1 are almost reached after 5 min. This suggests that the conversion of E to ES_1 is not affected by the replacement of Lys-59 by Gln. However, although the maximum of the curve for ES_2 appears between 100 and 200 s as observed with the wild-type enzyme, its amplitude is much larger due to an apparently slow conversion of ES_2 to ES_3 . As a result, the build-up of steady-state concentrations of the latter complexes is retarded.

The optimisation of the kinetic parameters for the simulation was more difficult in this case than described above for wild-type HMBS. Exact steady-state levels were not evident for ES_2 and ES_3 , even when additional measurements at up to 1 h were made. Furthermore, it proved to be impossible to obtain a steady-state proportion of ca. 0.1 for E, as evident from the measurements, without assuming that the preparation of $[\text{Gln}^{59}]\text{HMBS}$ contained ca. 10% of inactive enzyme. Such an unreactive protein fraction was expected to carry the net charge of active holoenzyme and would, therefore, be eluted together with the latter during chromatography. To test this hypothesis, the experiment with a contact time of 3 min was repeated several times and the material eluted with the first peak, expected to be a mixture of active and *enriched* inactive holoenzyme, was collected. Then, the combined fractions were subjected to the kinetic analysis at the same conditions (contact time 3 min). As anticipated, the peak corresponding to E was considerably larger in this case, reflecting the fact that inactive enzyme had not been turned over into ES_1 complexes. The increase in integrated peak area was used to estimate the contamination of the original enzyme preparation by inactive holoenzyme to be in the order of 4%.

A term reflecting the contamination was added to the rate equations by writing $[\text{E}]$ as $([\text{E}] - [\text{E}_d])$, where $[\text{E}_d] = dE_0/V_0$ ($0 < d < 1$) denotes the (constant) concentration of inactive holoenzyme. Regarding the trace for $[\text{ES}_1]$, the slow decrease of which seems to be coupled to the decrease of $[\text{ES}_2]$, the quality of the curve fitting could be slightly improved further by allowing $c_4 > 0$. A term that reflects a slow hydrolysis $\text{ES}_2 \rightarrow \text{ES}_1$ is, thereby, introduced. The curves shown in Fig. 2, c were eventually obtained by simplex optimisation of c_1 , c_3 , c_4 , c_5 , and c_{11} and d simultaneously (Table). The overall specificity constant derived from the simulation ($135 \text{ M}^{-1} \text{ s}^{-1}$) again compares favourably with the corresponding quantity measured in solution at the same conditions ($107 \text{ M}^{-1} \text{ s}^{-1}$).

The implications of this result with respect to the structure-function relationship in HMBS are considerable. In the crystal structure of HMBS, Lys-59 is located at one end of a flexible loop (residues 47–58) for which no well-defined electron density was observed [16]. Close examination of the structural model reveals that the side chain of Lys-59 is not

defined, suggesting that this residue, in addition to the loop, enjoys considerable flexibility. It was proposed that the loop may constitute a flexible lid with a role in transiently blocking access of solvent to the active site during catalysis, which may be important for protecting reactive intermediates [16]. The results presented here show that the role of the flexible loop is clearly not uniform in the sense that its task is the same for every elongation step. The presence of an aminobutyl side chain at residue 59 does not seem to matter for both the conversions $E \rightarrow ES_1$ and $ES_1 \rightarrow ES_2$, whereas it is obviously crucial for the transformations $ES_2 \rightarrow ES_3$ and $ES_3 \rightarrow E$. This differentiation possibly stems from a conformational change of HMBS during the reaction cycle. There are several independent indications for such changes. An increase of pK_1^E (representing apparent ionisations in free enzyme) to pK_1^{ES} (representing the corresponding ionisations in enzyme-substrate complexes) by 0.37 pH units on substrate binding presumably reflects a substrate-induced conformational change [17]. The fact that the reactivity of thiol groups of HMBS towards *N*-ethylmaleimide apparently increases as ES_1 , ES_2 , and ES_3 are formed suggests that cysteine side chains, buried in free holoenzyme, become exposed as the reaction proceeds [24]. A further indication, although indirect but perfectly compatible with the assumption that a substantial conformational change occurs on ES_2 binding the third PBG unit to form ES_3 , is the spacing of the corresponding peaks in the anion-exchange chromatogram (Fig. 1, *d*). Whereas the peaks representing E , ES_1 , and ES_2 are similarly spaced, there is a much larger separation of the peaks representing ES_2 and ES_3 , although the formal charge difference is the same in all cases [8].

[(SeMet)₆]HMBS. SeMet-Labelled proteins have recently gained considerable interest in X-ray-structural investigations, because the Se-atoms can serve as anomalous scatterers appropriate for the use of phasing methods based on MAD¹⁾ of synchrotron radiation [33]. It is of critical importance to perform thorough comparisons of [SeMet]proteins that are to be subjected to a MAD analysis and their wild-type counterparts, since the MAD analysis allows the high-resolution structure of a [SeMet]protein to be determined without the use of diffraction data from crystals of the wild-type protein [34]. It is, therefore, likely that three-dimensional structures of [SeMet]proteins will be exploited to uncover structure-function relationships.

The basic properties of [SeMet]HMBS are similar to those of wild-type HMBS, including the behaviour during purification, the overall steady-state kinetic parameters K_m and k_{cat} of purified material, and the habit of single crystals and their unit-cell dimensions [32]. It was interesting to see whether this similarity extends to individual specificity constants of the catalytic cycle. The results are presented in Fig. 2, *b* and the Table. Clearly, the overall specificity constant for this enzyme matches, within experimental error, the constant found for wild-type HMBS. This is in agreement with earlier results obtained from steady-state measurements at 37° in solution [32]. Regarding the relative individual specificity constants, however, there are slight but significant differences. Whereas c_3 (representing the conversion $ES_1 \rightarrow ES_2$), relative to c_1 , is somewhat smaller, c_5 vs. c_1 and c_{11} vs. c_1 are considerably larger than observed with wild-type enzyme. The same facts are reflected by different proportions of enzyme species at steady state for both enzymes (Fig. 2). Note that these proportions, and hence the relative specificity constants, are well reproducible for different batches of the same enzyme.

It is difficult to interpret these variations of the kinetics of the reaction mechanism upon replacement of S by Se-atoms in methionine residues, especially since the methion-

ine side chains do not seem to be directly involved with the structure of the active site in free holoenzyme [32]. There may be some significance in the fact that a qualitative change in behaviour (*i.e.*, smaller c_3 vs. c_1 as opposed to larger c_3 vs. c_1 and c_{11} vs. c_1) is again seen at the stage of ES_2 as it was observed with $[Gln^{59}]HMBS$, although with reversed sign. In this view, the presence of the Se-atoms would in some way facilitate the conformational change of ES_2 as it binds the third substrate, or, ES_2 being already in the new conformation, it would increase the second-order rate constant of the subsequent chain-elongation reactions.

We warmly thank Profs. Sir Alan Battersby and Kasper Kirschner for generous support and helpful discussions. The help of Drs. Philip Oliver, Chris Abell, and Peter Alefounder, University of Cambridge, with the construction of *E. coli* host strains and their transformation with suitable overexpression systems is gratefully acknowledged. Grateful acknowledgement is also made to the Treubel Fonds, Basel, Switzerland, to the Roche Research Foundation, to the Ciba-Geigy-Jubiläums-Stiftung, to the Stipendienfonds der Basler Chemischen Industrie, and to the Swiss National Science Foundation (projects 21-30264.90 and 20-35980.92) for financial support.

Experimental Part

1. *General.* Dithiothreitol, 2-amino-2-(hydroxymethyl)propane-1,3-diol (*Tris*) and PBG (**2**) were obtained from *Sigma*. A separate batch of **2** was kindly provided by Prof. A. R. Battersby. All other chemicals were of anal. reagent grade and were obtained from *Merck* or from *Fluka*. *NAP*-5, -10, and -25 columns were purchased from *Pharmacia*. The RAMSES software package [28] was obtained via anonymous internet file transfer ftp from the host *baikal.ethz.ch* (Internet address 129.132.80.130).

2. *Production and Characterisation of HMBS Enzymes.* 2.1. *Host Strains and Plasmids.* The system for the overexpression of wild-type and $[(SeMet)_6]HMBS$ from *E. coli* is based on the plasmid pPA410 carrying the *tac* promoter upstream of a 1.7 kb *Bam*HI-*Sal*I fragment of pLC41-4 [3] [13], containing the *hemC* gene (coding for HMBS) [35] [36]. The plasmid carrying the site-directed mutant variant of *hemC* for the production of $[Gln^{59}]HMBS$ is pPA448 [3]. The *E. coli* host strains used for overexpression of the enzymes were PO1423 (for wild-type and $[Gln^{59}]HMBS$) and the methionine auxotroph PO1562 (for $[(SeMet)_6]HMBS$) [32].

2.2. *Purification and Enzyme Assays.* The purification of overproduced enzymes involved, after sonication of the cells, a heat treatment, $(NH_4)_2SO_4$ fractionation, gel filtration, and anion-exchange chromatography. It was carried out following an established protocol [32]. Determinations of protein concentrations and assays of enzyme activity, both for monitoring of the purification and for steady-state kinetic analyses at 22° and at 37° (pH 7.4), were carried out as previously described [32]. Values of the steady-state parameters K_m and k_{cat} , as determined at 37°, matched those given in the literature within experimental error [3] [13] [32].

3. *Pre-Steady-State Kinetic Analysis.* 3.1. *Apparatus.* To run a *MonoQ*-HR-5/5 anion-exchange column from *Pharmacia*, either the FPLC system from *Pharmacia* or a *HP 1050* liquid chromatography system (*Ti* series) from *Hewlett-Packard* connected to a HPLC detector model 432 from *Kontron* was used. In either case, a *V-7* valve in connection with superloops (10 ml and 50 ml) from *Pharmacia* served as an injector. For on-line integration, an integrator model *HP 3396* series II from *Hewlett-Packard* was used.

3.2. *Buffer System.* Buffer *A*: 15 mM *Tris*·HCl pH 7.5, 0.6 mM ethylenediaminetetraacetic acid, 0.1 mM dithiothreitol. Buffer *B*: 350 mM NaCl in buffer *A*.

3.3. *Solution of Substrate.* A soln. of PBG (1.46 μ M) in *A/B* 3:1 was set up in one of the superloops (10 ml or 50 ml) of the FPLC system. To avoid errors in contact time, the filled loop was checked to be free of any air bubbles, and the tubing leading to the injector was filled with PBG soln. as well.

3.4. *Immobilisation of HMBS.* A sample of HMBS, as obtained after the final purification step (anion-exchange chromatography at pH 6.0), was subjected to exchange in *A/B* 3:1 using a *NAP* column of suitable size. Then, the equivalent to 0.10 mg of enzyme was injected onto *MonoQ* HR 5/5 using a 500- μ l sample loop, *A/B* 3:1 as mobile phase, and a flow rate of 3 ml/min. It was essential to avoid the presence of any trace amounts of PBG during this step by carefully washing the injection valve with mobile phase beforehand.

3.5. *Generation of Enzyme-Substrate Complexes.* The column loaded with HMBS was equilibrated with 25% *B* at 3 ml/min for 1 min. This time interval was used to attach the superloop with the PBG soln. to the injector. Then, without interrupting the flow, the experiment was started by switching the valve to position 'inject'. After a time

interval (contact time) which was varied, the valve was switched back to 'load', and at the same time, the flow rate was reduced to 1 ml/min and a pre-programmed gradient (25–100% *B* in 30 min) was started to elute and separate free enzyme and the enzyme-substrate complexes. The species were detected at 280 nm and their proportions determined. Each of the measurements shown in Fig. 2 represents the average proportions and the corresponding standard deviations of data from 3 independent determinations. Control experiments in which *A/B* 3:1 replaced the PBG soln. gave rise to a single peak representing free enzyme.

3.6. Determination of Product as Uroporphyrin I. After elution of the ES_3 complex, the column was reversed. The product was eluted by repeatedly eluting 500- μ l portions of 2M NaCl, in elution volumes of 750 μ l, into 750- μ l portions of 7% aq. CCl_3COOH soln. Of a soln. of 0.5% I_2 in 1.0% KI, 400 μ l were added to each of the samples, as were, after at least 3 min, 100 μ l of 2% $Na_2S_2O_3$ soln. The porphyrin content was determined by measuring the absorption at 406 nm using $\epsilon_{406} = 528'000 \text{ l mol}^{-1} \text{ cm}^{-1}$ [37]. In a control experiment carried out as specified above but with loading buffer soln. instead of enzyme, it was found that there is no contributing absorption at 406 nm arising from PBG soln. alone.

3.7. Estimation of the Relative Velocity of Mobile Phase. The height of a 1-ml volume in an empty *HR 5/5* column is $1 \text{ cm}^3 / (0.25^2 \text{ cm}^2 \pi) = 5.1 \text{ cm}$. Since *MonoQ* beads have void volumes of 40% (i.e. 60% of space is occupied by the particles), the height for 1 ml of void volume is 12.7 cm. At a flow rate of 1 ml/min, the velocity of the fluid relative to the bead is ca. 0.21 cm s^{-1} .

3.8. Computer Simulation. To quantify free enzyme, the enzyme-substrate complexes, substrate, and product in units of concentration, it was assumed that free enzyme, as it is loaded on *MonoQ HR 5/5*, occupies some formal volume V_0 on the column ($0 < V_0 < 390 \mu\text{l}$). Furthermore, it was assumed that the enzyme-substrate complexes and the product, as they are formed, remain contained within V_0 . These assumptions allowed the differential Eqns. 1–6 to be used directly within the ModelWorks programming environment [27] provided by the RAMSES software [28]. An elementary step of the simulation, the time of which is governed by F and V_0 , then involves replacing the existing soln. contained in V_0 by an equivalent volume of fresh soln. being [PBG] in substrate and calculating the changes of concentrations of species according to the differential equations. To handle the substrate concentration within V_0 , terms describing the supply ($F[\text{PBG}]/V_0$) and removal ($F\sigma[S]/V_0$) of substrate with the mobile phase are present apart from terms related to the reaction of substrate with the enzyme species (see Eqn. 5). The presence of the factor σ is necessary since PBG is slightly retained by *MonoQ* at the specified conditions. The retention volume of PBG, measured in unities of void volume, can be shown to be $1/\sigma$ as follows. We assume that the column has N formal volumes numbered V_n ($n = 0, 1, \dots, (N-1)$). Another formal volume V_N , representing a detector, is added at the end of the column. Starting with a concentration unity in formal volume V_0 , we distribute concentrations between V_n and V_{n+1} with factors $(1-\sigma)$ and σ , respectively, in discrete steps m ($m = 0, 1, \dots, (N-1), N, (N+1), \dots$). The concentration c_{nm} in V_n at step m is given by Eqn. 11.

$$c_{nm} = \binom{m}{n} \sigma^n (1-\sigma)^{m-n} \quad (11)$$

In particular, $c_{nm} = 0$ for $n > m$, $c_{nm} = \sigma^n$ for $n = m$, $c_{00} = 1$, and $c_{0m} = (1-\sigma)^m$. Since m is a measure of retention volume, we can normalise the retention volumes to unities of the void volume. For a compound with $\sigma = 1$, it takes $m = N$ steps to detect the compound in V_N , since $c_{nm} = 1$ and $c_{Nm} = 0$ for $m \neq N$. Therefore, the normalised retention volume is m/N and the void volume is $1 (N/N)$. For a compound with $0 < \sigma < 1$, we will detect c_{Nm} (Eqn. 12).

$$c_{Nm} = \binom{m}{N} \sigma^N (1-\sigma)^{m-N} \text{ for all steps } m > N \quad (12)$$

The latter compound will have a normalised retention volume $x > 1$. Given $x = m/N$, we determine the value of σ for which the function c_{Nm} is a maximum. After setting the derivative of c_{Nm} equal to 0, we get $x = 1/\sigma$.

The actual simulation programme was implemented within ModelWorks as a Modula-2 [29] module and run on a *Macintosh IIfx* computer. The source code of the module, a detailed description of which will be reported elsewhere, can be obtained from the authors. The module includes a procedure for unattended χ^2 optimisation of selected parameters using the downhill simplex algorithm which is implemented according to the procedure *amoeba* by Press *et al.* [30]. Reasonable starting values for the parameters to be optimised were derived from the steady-state proportions of enzyme species in combination with a coarse manual adjustment of c_1 (wild-type and $[(\text{SeMet})_6]\text{HMBS}$). In the case of $[\text{Gln}^{59}]\text{HMBS}$, the apparent first-order conversion of ES_2 to ES_3 was used to estimate c_5 . The latter as well as c_1 and c_3 (taken from wild-type HMBS) being kept constant, c_{11} was manually adjusted to get the starting values for the optimisation. Typically, an optimisation required 100–400 simulation runs.

REFERENCES

- [1] A. R. Battersby, C. J. R. Fookes, G. W. J. Matcham, E. McDonald, *Nature (London)* **1980**, 285, 17.
- [2] P. M. Jordan, in 'Biosynthesis of Tetrapyrroles', Ed. P. M. Jordan, Elsevier, Amsterdam, 1991, p. 1.
- [3] A. Hädener, P. R. Alefounder, G. J. Hart, C. Abell, A. R. Battersby, *Biochem. J.* **1990**, 271, 487.
- [4] D. C. Williams, G. S. Morgan, E. McDonald, A. R. Battersby, *Biochem. J.* **1981**, 193, 301.
- [5] A. R. Battersby, C. J. R. Fookes, G. Hart, G. W. J. Matcham, P. S. Pandey, *J. Chem. Soc., Perkin Trans. 1* **1983**, 3041.
- [6] G. J. Hart, A. D. Miller, F. J. Leeper, A. R. Battersby, *J. Chem. Soc., Chem. Commun.* **1987**, 1762.
- [7] P. M. Jordan, M. J. Warren, *FEBS Lett.* **1987**, 225, 87.
- [8] G. J. Hart, A. D. Miller, U. Beifuss, F. J. Leeper, A. R. Battersby, *J. Chem. Soc., Perkin Trans. 1* **1990**, 1979.
- [9] P. M. Anderson, R. J. Desnick, *J. Biol. Chem.* **1980**, 255, 1993.
- [10] A. R. Battersby, C. J. R. Fookes, G. W. J. Matcham, E. McDonald, R. Hollenstein, *J. Chem. Soc., Perkin Trans. 1* **1983**, 3031.
- [11] P. M. Jordan, S. D. Thomas, M. J. Warren, *Biochem. J.* **1988**, 154, 427.
- [12] G. J. Hart, A. D. Miller, A. R. Battersby, *Biochem. J.* **1988**, 252, 909.
- [13] M. Lander, A. R. Pitt, P. R. Alefounder, D. Bardy, C. Abell, A. R. Battersby, *Biochem. J.* **1991**, 275, 447.
- [14] A. R. Battersby, C. J. R. Fookes, G. W. J. Matcham, E. McDonald, *J. Chem. Soc., Chem. Commun.* **1979**, 539.
- [15] P. M. Jordan, S. C. Woodcock, *Biochem. J.* **1991**, 280, 445.
- [16] G. V. Louie, P. D. Brownlie, R. Lambert, J. B. Cooper, T. L. Blundell, S. P. Wood, M. J. Warren, S. C. Woodcock, P. M. Jordan, *Nature (London)* **1992**, 359, 33.
- [17] G. J. Hart, C. Abell, A. R. Battersby, *Biochem. J.* **1986**, 240, 273.
- [18] A. Rosevear, J. F. Kennedy, J. M. S. Cabral, in 'Immobilised Enzymes and Cells', Adam Hilger, Bristol, Philadelphia, 1987, p. 148.
- [19] A. Fersht, 'Enzyme Structure and Mechanism', Freeman, New York, 1985.
- [20] J. A. Nelder, R. Mead, *Computer J.* **1965**, 7, 308.
- [21] M. W. Routh, P. A. Swartz, M. B. Denton, *Anal. Chem.* **1977**, 49, 1422.
- [22] A. Cornish-Bowden, C. W. Wharton, 'Enzyme Kinetics', IRL Press, Oxford, 1988.
- [23] P. M. Jordan, in 'The Biosynthesis of the Tetrapyrrole Pigments', Eds. D. J. Chadwick and K. Ackrill, Wiley, Chichester, 1994, p. 70.
- [24] M. J. Warren, P. M. Jordan, *Biochemistry* **1988**, 27, 9020.
- [25] A. R. Battersby, C. J. R. Fookes, G. W. J. Matcham, E. McDonald, K. E. Gustafson-Potter, *J. Chem. Soc., Chem. Commun.* **1979**, 316.
- [26] A. R. Battersby, C. J. R. Fookes, K. E. Gustafson-Potter, E. McDonald, G. W. J. Matcham, *J. Chem. Soc., Perkin Trans. 1* **1982**, 2427.
- [27] A. Fischlin, D. Gyalistras, O. Roth, M. Ulrich, J. Thöny, T. Nemecek, H. Bugmann, F. Thommen, 'Model-Works. An Interactive Simulation Environment for Personal Computers and Workstations. Version 2.2', Systems Ecology, Institute of Terrestrial Ecology, Department of Environmental Sciences, Swiss Federal Institute of Technology, Grabenstrasse 3, CH-8952 Schlieren, Zürich, 1994.
- [28] A. Fischlin, 'Research Aids for Modelling and Simulation of Environmental Systems (RAMSES)', Systems Ecology and ETH Zürich, Zürich, 1993.
- [29] N. Wirth, 'Programming in Modula-2', Springer Verlag, Berlin-Heidelberg, 1985.
- [30] W. H. Press, B. P. Flannery, S. A. Teukolsky, W. T. Vetterling, 'Numerical Recipes in Pascal', Cambridge University Press, Cambridge, UK, 1989.
- [31] A. I. Scott, C. A. Roessner, N. J. Stolowich, P. Karuso, H. J. Williams, S. K. Grant, M. D. Gonzalez, T. Hoshino, *Biochemistry* **1988**, 27, 7984.
- [32] A. Hädener, P. K. Matzinger, V. N. Malashkevich, G. V. Louie, S. P. Wood, P. Oliver, P. R. Alefounder, A. R. Pitt, C. Abell, A. R. Battersby, *Eur. J. Biochem.* **1993**, 211, 615.
- [33] W. A. Hendrickson, J. R. Horton, D. M. LeMaster, *EMBO J.* **1990**, 9, 1665.
- [34] W. Yang, W. A. Hendrickson, R. J. Crouch, Y. Satow, *Science* **1990**, 249, 1398.
- [35] P. R. Alefounder, C. Abell, A. R. Battersby, *Nucleic Acids Res.* **1988**, 16, 9871.
- [36] S. D. Thomas, P. M. Jordan, *Nucleic Acids Res.* **1986**, 14, 6215.
- [37] C. Rimington, *Biochem. J.* **1960**, 75, 620.